ARL-TR-7814 ● SEP 2016

US Army Research Laboratory

# Development of Photoacoustic Sensing Platforms at the US Army Research Laboratory

by Ellen L Holthoff and Paul M Pellegrino

## NOTICES

### Disclaimers

The findings in this report are not to be construed as an official Department of the Army position unless so designated by other authorized documents.

Citation of manufacturer's or trade names does not constitute an official endorsement or approval of the use thereof.

Destroy this report when it is no longer needed. Do not return it to the originator.

ARL-TR-7814 ● SEP 2016

US Army Research Laboratory

# Development of Photoacoustic Sensing Platforms at the US Army Research Laboratory

**by Ellen L Holthoff and Paul M Pellegrino**
*Sensors and Electron Devices Directorate, ARL*

# REPORT DOCUMENTATION PAGE

*Form Approved*
*OMB No. 0704-0188*



| 1. REPORT DATE *(DD-MM-YYYY)* | 2. REPORT TYPE | 3. DATES COVERED (From - To) |
|---|---|---|
| September 2016 | Technical Report | |

**4. TITLE AND SUBTITLE**
Development of Photoacoustic Sensing Platforms at the US Army Research Laboratory

**5a. CONTRACT NUMBER**

**5b. GRANT NUMBER**

**5c. PROGRAM ELEMENT NUMBER**

**6. AUTHOR(S)**
Ellen L Holthoff and Paul M Pellegrino

**5d. PROJECT NUMBER**

**5e. TASK NUMBER**

**5f. WORK UNIT NUMBER**

**7. PERFORMING ORGANIZATION NAME(S) AND ADDRESS(ES)**
US Army Research Laboratory
ATTN: RDRL-SEE-E
2800 Powder Mill Road
Adelphi, MD 20783-1138

**8. PERFORMING ORGANIZATION REPORT NUMBER**
ARL-TR-7814

**9. SPONSORING/MONITORING AGENCY NAME(S) AND ADDRESS(ES)**

**10. SPONSOR/MONITOR'S ACRONYM(S)**

**11. SPONSOR/MONITOR'S REPORT NUMBER(S)**

**12. DISTRIBUTION/AVAILABILITY STATEMENT**
Approved for public release; distribution unlimited.

**13. SUPPLEMENTARY NOTES**

**14. ABSTRACT**
Traditionally, chemical sensing platforms have been hampered by the opposing concerns of increasing sensor capability while maintaining a minimal package size. Current sensors, although reasonably sized, are geared to more classical chemical threats, and the ability to expand their capabilities to a broader range of emerging threats is uncertain. Recently, photoacoustic spectroscopy, employed in a sensor format, has shown enormous potential to address these ever-changing threats. Photoacoustic spectroscopy is one of the more flexible IR spectroscopy variants, and that flexibility allows for the construction of sensors that are designed for specific tasks. The US Army Research Laboratory has, for the past 14 years, engaged in research into the development of photoacoustic sensing platforms with the goal of sensor miniaturization and the detection of a variety of chemical targets both proximally and at range. This report reviews this work.

**15. SUBJECT TERMS**
photoacoustic sensing, quantum cascade laser, chemical detection, standoff, microelectromechanical system, MEMS

| 16. SECURITY CLASSIFICATION OF: | | | 17. LIMITATION OF ABSTRACT | 18. NUMBER OF PAGES | 19a. NAME OF RESPONSIBLE PERSON |
|---|---|---|---|---|---|
| a. REPORT | b. ABSTRACT | c. THIS PAGE | | | Ellen L Holthoff |
| Unclassified | Unclassified | Unclassified | UU | 40 | 19b. TELEPHONE NUMBER (Include area code) 301-394-0939 |

## Contents

## List of Figures

## Acknowledgments

We acknowledge David Heaps, John Schill, and Logan Marcus for their efforts and participation in various aspects of this research, and the contributions of Nancy Stoffel, William Benard, William Potter, Brain Cullum, and Mikella Farrell.

# 1. Introduction

In recent years, photoacoustic spectroscopy (PAS) has emerged as an attractive and powerful technique well suited for sensing applications. The development of high-power radiation sources and more sophisticated electronics, including sensitive microphones and digital lock-in amplifiers, have allowed for significant advances in PAS.[1,2] Furthermore, photoacoustic (PA) detection of IR absorption spectra using modern tunable lasers offers several advantages, including simultaneous detection and discrimination of numerous molecules of interest. Successful applications of PAS in gases and condensed matter have made this a notable technique and it is now studied and employed by scientists and engineers in a variety of disciplines.

PAS is a detection technique under the umbrella of photothermal spectroscopy. Photothermal spectroscopy encompasses a group of highly sensitive methods that can be used to detect trace levels of optical absorption and subsequent thermal perturbations of the sample in gas, liquid, or solid phases. The underlying principle that connects these various spectroscopic methods is the measurement of physical changes (i.e., temperature, density, or pressure) as a result of a photo-induced change in the thermal state of the sample. Other photothermal techniques include photothermal interferometry (PTI), photothermal lensing (PTL), and photothermal deflection (PTD). All photothermal processes consist of several linked steps that result in a change of the state of the sample. In general, the sample undergoes an optical excitation, which can take various forms of radiation, including laser radiation. This radiation is absorbed by the sample placing it in an excited state (i.e., increased internal energy). Some portion of this energy decays from the excited state in a nonradiative fashion. This increase in local energy results in a temperature change in the sample or the coupling fluid (e.g., air). The increase in temperature can result in a density change and, if it occurs at a faster rate than the sample or coupling fluid can expand or contract, the temperature change will result in a pressure change. As mentioned, all photothermal methods attempt to key in on the changes in the thermal state of the sample by measuring the index of refraction change as with PTI, PTL, and PTD; temperature change as with photothermal calorimetry and photothermal radiometry; or pressure change as with PAS.[3]

In order to generate acoustic waves in a sample, periodic heating and cooling of the sample is required to produce pressure fluctuations. This is accomplished using modulated or pulsed excitation sources.[4–6] The pressure waves detected in PAS are generated directly by the absorbed fraction of the modulated or pulsed excitation beam. Therefore, the signal generated from a PA experiment is directly proportional to the absorbed incident power. However, depending on the type of excitation

source (i.e., modulated or pulsed), the relationship between the generated acoustic signal and the absorbed power at a given wavelength will differ.[7,8] There are 2 main categories of light sources used for PAS: broadband sources and narrowband laser sources. Although lamp-based PAS is still common, modern PAS research has been mainly performed using laser sources.

In 1994 the introduction of the quantum cascade laser (QCL) by Bell Labs[9] changed the prospects of laser PA and, in general, IR spectroscopy. Since that time, continuing and aggressive evolution has been occurring. The QCL has matured to a level at which numerous companies can produce gain material for laser systems both in the United States and abroad. Along with this production, several companies have produced laser systems that are suitable for spectroscopic purposes (e.g., Daylight Solutions, Inc.; Pendar Technologies; Pranalytica, Inc.; and Block Engineering), allowing for continuous wavelength tuning ranges of greater than or equal to 200 $cm^{-1}$. The resolution of well-constructed systems can tune continuously and without mode-hoping over the whole tuning band with a nominal resolution of approximately 1 $cm^{-1}$. Power output of spectroscopic sources has generally been moderate; 10s of milliwatt average power and on the order of 100s of milliwatt peak pulsed power. Furthermore, QCLs, operating in low duty cycles, have demonstrated that PAS based on lock-in amplification can still be performed and indeed shows great promise.

There are numerous publications with thorough discussions on the use of PAS for various applications,[7,10–14] and although studies have demonstrated the sensitivity capabilities of PA sensors, the total system size represents a large logistics burden in terms of size, cost, and power consumption.[1,2] For the past 14 years, the US Army Research Laboratory (ARL) has engaged in a wide-ranging effort to develop novel PA sensing platforms that address the challenges of chemical sensing for Army applications. We have focused on gas sensor miniaturization and the application of QCL technology in our PA sensor platforms. In addition, a theoretical method for predicting the resonant frequency of PA cells with side branches has been developed. This report reviews PA sensor development and demonstrations at ARL. The majority of these results have been discussed previously[15–18]; however, it is important to highlight them again for the purpose of this report.

## 2. Photoacoustic Sensing of Gaseous Samples

Investigations of gaseous species continue to be the most common application for PAS. Figure 1 depicts a block diagram of the main components in the ARL PA gas sensor system. A laser excitation source is either modulated or pulsed and directed at a PA cell, which serves as a container for the sample as well as the detector. The

resultant pressure wave, which is created due to sample heating, is detected by a microphone having the appropriate frequency response. Although alternative methods of transduction have been demonstrated,[19–21] the microphone is the most widely used pressure sensor for PA applications. The signal generated by the microphone is proportional to the amplitude of the pressure wave, but other information is contained in the phase and delay of the wave as well. This information is captured by lock-in amplification. The sample cell is a resonant chamber. Trace gases are generated using a calibration gas generator. Nitrogen is used as the carrier gas and the gas sources are gravimetrically certified permeation tubes. Varying calibrated flow rates of the nitrogen carrier gas governs the concentration of the analytes of interest. The concentration range for each analyte is limited by the permeation tube and the permissible flow rates of the calibration gas generators. A flow controller and a relief valve are placed in line between the gas generator and the PA cell to ensure a constant flow rate through the cell to reduce flow noise. A PC is used to read and record the voltage outputs from the lock-in amplifier and a power meter is employed to measure the transmitted laser power, which allows for normalization of the PA signal for any residual drift associated with the excitation source.

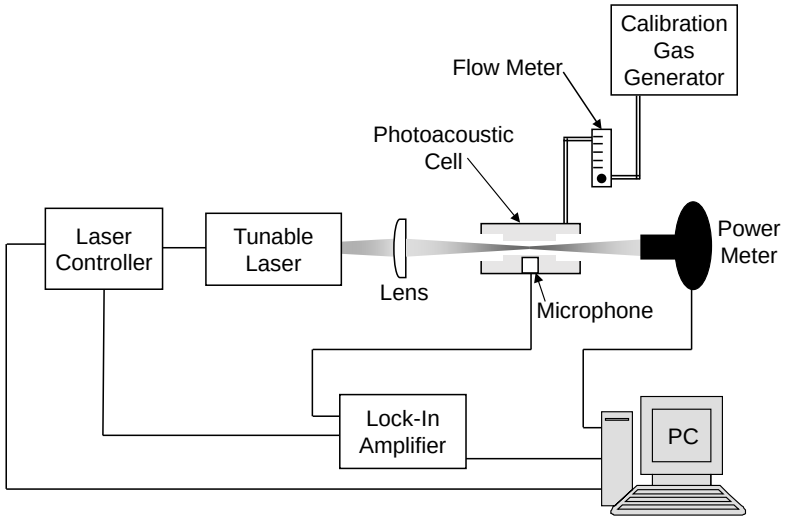


**Fig. 1 Simplified schematic diagram of the ARL laser-based photoacoustic gas sensor system**

## 2.1 Laser Source

Over the past 10 years, ARL has evaluated QCL technology in the implementation of these sources in our PA gas sensor platforms. We have employed a variety of external cavity (EC) QCLs, including pulsed, modulated continuous wave (CW),

and quasi-continuous wave (Q-CW) (i.e., high duty cycle pulsed operation, typically ~50%) sources, with broad tunability across different wavelength regions in the IR. The Q-CW laser produced a train of pulses at a high repetition rate (1 MHz). An external modulation envelope could be applied to the train of pulses producing modulated packets of pulses. Alternatively, the laser could be driven externally to produce pulses at lower repetition rates (down to 10s of Hz). ARL has also evaluated a prototype laser developed during an Army Small Business Innovation Research Phase II Development program. The compact source built for this program offers performance in a small package (a 2-inch cube) that is typically achieved with larger, bench-top laboratory QCLs. The packaged laser prototype contained a voice coil motor-based tuning mechanism that allowed both sweeping and stepping motions for rapid wavelength tunability.

## 2.2 Acoustic Resonators

An essential element of a PA gas sensor is the cell, most commonly a cylindrical tube resonator, which serves as a container for the sample as well as the detector. Therefore, optimum design of a PA cell is necessary to facilitate signal generation and detection.[1,14,22–24] In conjunction with research to examine performance and design issues associated with the miniaturization of PA cells, we fabricated and tested a miniature non-microelectromechanical systems (MEMS) (macro) cell.[25] The basic design for the macro PA cell is a modified version of the cell studied by Bijnen et al.[1] Numerous approaches to optimize a PA cell for trace gas detection were investigated, resulting in suggested parameters for the construction of a sensitive resonant cell with a fast response time. Our design is a ¼ scale down from the "Bijnen" cell, with a resonator radius ($r_{res}$) = 0.75 mm and resonator length ($l_{res}$) = 30 mm. Experimental results suggested that miniaturization of a PA cell is viable without a significant loss in signal and no adverse effects of the size scaling were visualized in the optics or acoustics of the macro cell. We achieved a detection limit of 65 parts-per-trillion (ppt) for sulfur hexafluoride using this macro cell.

Initial examination of the scaling principles associated with PAS with respect to MEMS dimensions indicated that PA signals would remain at similar sensitivities or even surpass those commonly found in macroscale devices.[25–30] The MEMS-based PA sensor platforms designed by ARL for trace gas detection have used modified versions of the differential PA cell developed by Miklós.[31] The differential technique employs 2 resonator tubes, both housing a microphone, but with radiation directed only through one to generate a PA signal. The microphones possess similar responsivities, which allow for subtraction of the reference microphone signal from the PA microphone signal. This allows for the removal of

noise elements that are present in both resonant chambers, such as external vibrations. Figure 2 includes a photograph of the internal structure of our MEMS-scale version of the "Miklós" cell and the complete PA cell package. The resonators have square cross sections with $l_{res}$ = 8.5 mm and $r_{res}$ = 0.465 mm. Buffer volumes in the cell structure act as acoustic filters to suppress window and gas flow noise. The cell had 2 germanium (Ge) windows, which were attached to buffer volumes on either side of the resonator with epoxy. Tygon tubing was connected to the buffer volumes to allow for gas sample inlet and outlet flow. The MEM-scale PA cell was mounted on a printed circuit board, which allowed for wiring the microphones to a power supply (AA battery) and a lock-in amplifier (via modified BNC cables). Another MEMS cell design consisted of 2 open resonators having square cross sections ($l_{res}$ = 10 mm), each with $r_{res}$ = 0.432 mm. The resonator is flanked on both sides by a buffer volume. To further suppress gas flow noise, the cell had a convoluted, split sample inlet/outlet design.[16] For each of these MEMS-scale PA cell designs, resonator and buffer volume dimensions were determined based on the criteria presented for the "Bijnen" cell.

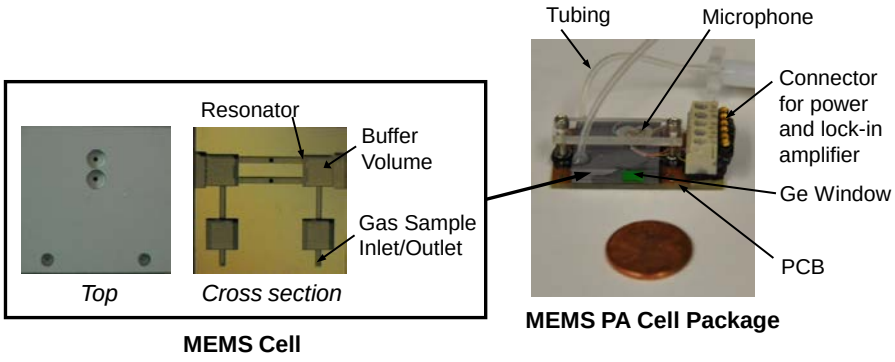


**Fig. 2 Photograph of the internal structure of the MEMS-scale cell and complete PA cell package**

There are numerous examples in the literature of PA cells designs for pulsed PAS applications.[32–35] The authors suggest cell designs that differ from those used for modulated PAS. The MEMS-scale PA cell designs developed by ARL for our PA trace gas sensors have been used effectively for both modulated and pulsed sources.

As is often the case for trace gas sensing, the detection sensitivity is limited by the ratio of signal to noise (SNR). Applying higher modulation frequencies and acoustic amplification of the PA signal will result in an improved SNR. When the modulation or pulse frequency is the same as an acoustic resonance frequency of the PA cell, the resonant eigenmodes (i.e., acoustic modes) of the cell can be excited, resulting in an amplification of the signal.[36–38] The resonance frequencies are dependent on the shape and size of the PA cell. The fundamental resonant mode

of a cylindrical resonator is related to resonator length and a basic "rule of thumb" is applied in the literature to predict this frequency value.[1,39] Although the MEMS-scale PA cells designed at ARL were based on parameters offered in the literature, the acoustics did not agree with frequency predictions. Bijnen offered a brief explanation for altered acoustic behavior due to the influence of a small connecting channel (i.e., side branch) located between the resonator tube and the opening for the microphone,[1] but the significant effect the length of the side branch and the diameter of the side branch hole have on the resonant frequency of the tube resonator were not clearly addressed.

ARL has demonstrated the critical effect the diameter of a side branch hole has on the resonant frequency of a tube resonator.[40] This effect should not be overlooked in the design of PA cells with similar geometrical features. We introduced a theoretical method for predicting the resonant frequencies of acoustic resonators with side branches. The derived resonance conditions, which consider the input impedance to the side branch structure of a PA cell, significantly improve the ability to predict the cell resonant frequency. This method has been successfully extended to MEMS-scale PA cell resonators with complex side branch structures.

## 2.3 Application

ARL has collected PA spectra and limits of detection (LODs) for various analytes of interest using our MEMS-scale PA sensor platforms and employing a variety of EC-QCLs as excitation sources. Figure 3 shows the PA spectra for the standard nerve agent stimulant, dimethyl methyl phosphonate (DMMP), collected using our PA gas sensor.[16] The spectrum in Fig. 3a was collected as a pulsed Daylight Solutions QCL and was continuously tuned from 990 to 1075 $cm^{-1}$ (10.10 to 9.30 μm), in 1-$cm^{-1}$ increments. DMMP has known absorption features in this wavelength range, assigned to phosphorus–oxygen–carbon stretching vibrations. The source operated at room temperature with passive air cooling and a 20.9-kHz pulse rate provided an average optical power of 1.35 mW. The spectrum in Fig. 3b was collected as a modulated CW Daylight Solutions QCL and was continuously tuned from 1032 to 1070 $cm^{-1}$ (9.69–9.34 μm). Due to the mode hopping[41] nature of this source, we reduced the number of measured wavelengths, which was possible due to the broad absorption features of DMMP in this wavelength region. The source required a compact chiller for cooling. An injection current of 725 mA provided an average optical power of 11.97 mW. A function generator was connected to the laser head via a subminiature version A connector to allow for external current modulation. A 17.2-kHz sine wave with a peak amplitude of 2.5 V resulted in 65% amplitude modulation. The absorbance spectrum for DMMP,

which was recorded using a Fourier transform IR (FTIR), is also provided in Fig. 3a and b for comparison to the PA data. There is good agreement between the laser PA data and the FTIR spectroscopy absorbance spectrum.

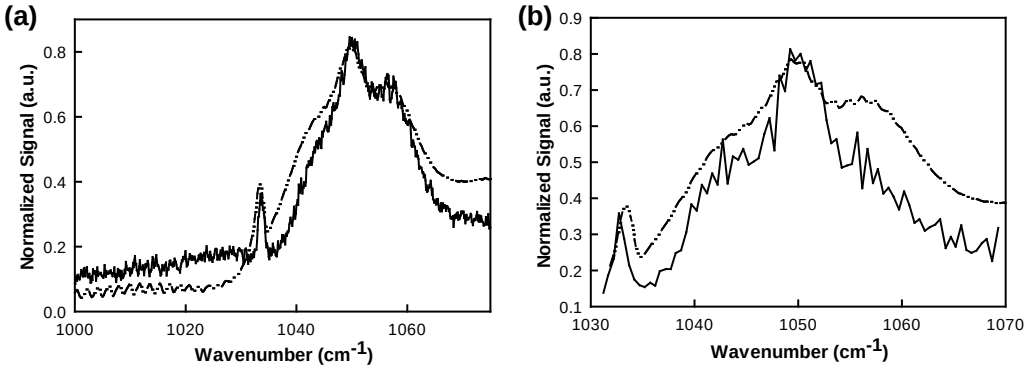


**Fig. 3 Measured a) pulsed and b) modulated CW laser PA spectra (—) of DMMP. Data derived from our own PA measurements are compared to FTIR reference spectrum (– ·· –).**

The DMMP absorbance maximum in the QCL wavelength tuning range is 1053 $cm^{-1}$ (9.50 μm). Therefore, this wavelength is best suited for continuous DMMP sensitivity monitoring. The sensor response as a function of DMMP concentration at the absorbance maximum was measured and the results exhibited excellent linearity. Minimal detectable DMMP concentrations of 54 parts-per-billion (ppb) and 20 ppb were achieved with the pulsed QCL and modulated CW QCL-based PA sensor systems, respectively.

We employed a different QCL in our PA sensing system to study chlorobenzene, a propellant analog and an intermediate in the manufacture of certain pesticides (e.g., DDT), and hexafluoroethane (Freon 116), also a propellant analog and a component in refrigerants.[42] Figure 4 shows the spectra of chlorobenzene and Freon 116 collected as a pulsed Daylight Solutions QCL was continuously tuned from 1050 to 1240 $cm^{-1}$ (9.52 to 8.06 μm), in 1-$cm^{-1}$ increments. Both species have known absorption features in this spectral region, assigned to carbon–carbon stretch frequencies in the chlorobenzene molecules and carbon–fluorine stretching vibrations in the Freon 116 molecules. The pulsed source operated at room temperature with passive air cooling. A 21.6-kHz pulse rate provided an average optical power of 1.32 mW. The absorbance spectra for these species, recorded using an FTIR spectrometer, are also provided in Fig. 4 for comparison to the PA data. There is excellent agreement between the PA and FTIR spectroscopy data. The sensor response as a function of chlorobenzene and Freon 116 concentrations was measured and the results exhibited excellent linearity. We achieved a minimal

detectable chlorobenzene concentration of 162 ppb and a minimal detectable Freon 116 concentration of 19 ppb.

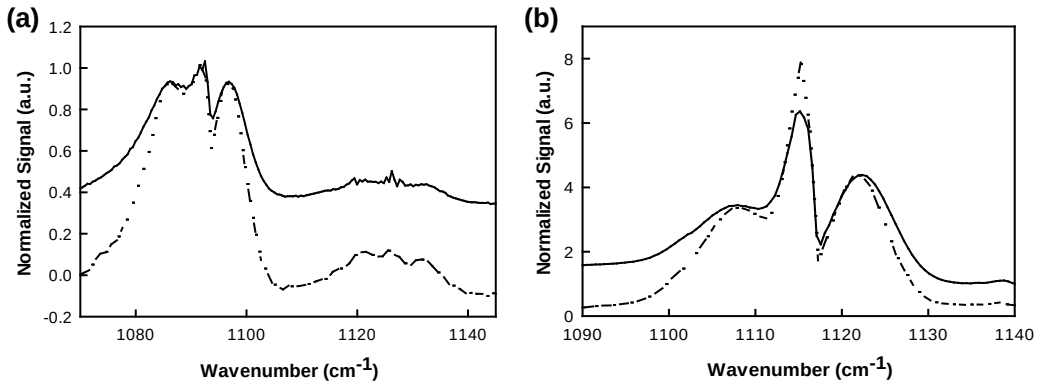


**Fig. 4 Measured pulsed laser PA spectra of a) chlorobenzene (—) and b) Freon 116 (—). Data derived from our own PA measurements are compared to FTIR reference spectra (– –).**

Although commercially available QCLs are more compact in comparison to other popular IR sources used for PAS (i.e., carbon dioxide [$CO_2$] lasers), they are still rather large in relation to MEMS-scale components. To realize the advantage of PA sensor miniaturization, light sources of comparable size are required. ARL has reported on the use of a broadly tunable, ultracompact, pulsed EC-QCL (SpriteIR) developed by Daylight Solutions.[43] This laser system (i.e., laser head and controller) was approximately one tenth the size of a standard commercially available, broadly tunable EC-QCL system from Daylight Solutions. Photographs of the packaged laser and controller prototypes are shown in Fig. 5.

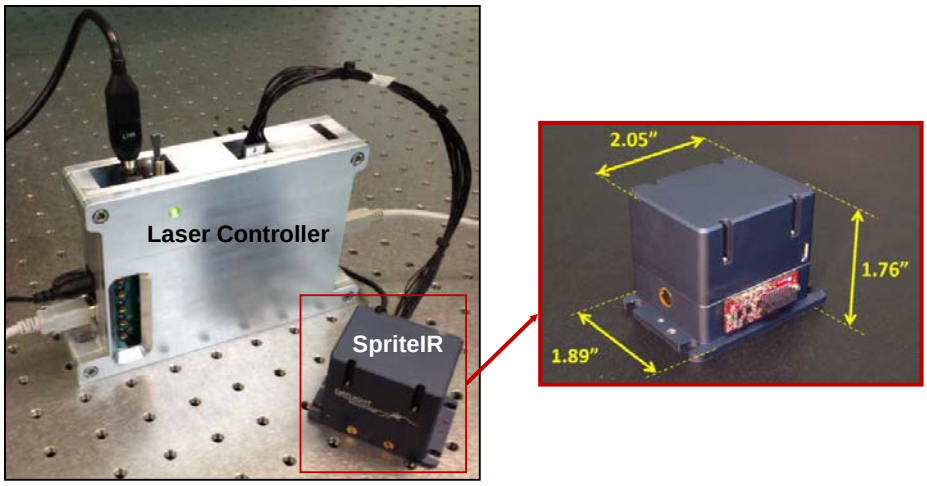


**Fig. 5 Photographs of the packaged laser and controller prototypes, including the dimensions of the packaged SpriteIR laser module**

SpriteIR was used in combination with a MEMS-scale PA cell design for detection of 1,4-dioxane. The spectrum of this analyte is shown in Fig. 6 and was collected as the laser was continuously tuned from 1100 to 1170 $cm^{-1}$ (9.09 to 8.55 μm), in 1-$cm^{-1}$ increments. 1,4-Dioxane has known absorption features in this region, assigned to carbon–carbon and carbon–oxygen stretching vibrations. The prototype pulsed source was mounted on a cooling tower and required a compact chiller for operation at 17 °C. A 20.0-kHz pulse rate resulted in an average optical power of 1.08 mW. The absorbance spectrum for 1,4-dioxane, recorded using an FTIR spectrometer, is also provided in Fig. 5 for comparison to the PA data. A PA spectrum of 1,4-dioxane collected using a commercially available Daylight Solutions EC-QCL is also provided in Fig. 6 for comparison.[15] There was excellent agreement between the spectra. The 1,4-dioxane absorbance maximum in the QCL wavelength tuning range is 1138 $cm^{-1}$ (8.78 μm). The sensor response as a function of 1,4-dioxane concentration at the absorbance maximum was measured and the results exhibited excellent linearity. We achieved a minimal detectable 1,4-dioxane concentration of 133 ppb. Our reported LOD for 1,4-dioxane using a similar MEMS-scale PA sensor platform, in which we employed a commercially available pulsed EC-QCL, was 180 ppb.[15] Although the average power output of the SpriteIR laser was less than that of the commercial source, we observed less noise or background signal using the SpriteIR laser, which allowed for an improved detection limit.

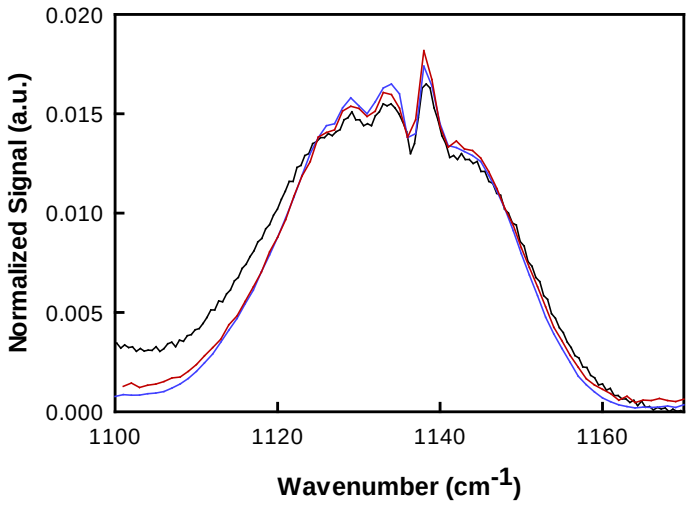


**Fig. 6 Measured SpriteIR laser PA spectrum of 1,4-dioxane (red) compared to FTIR reference spectrum (black) and commercially available EC-QCL PA spectrum (blue)**

As discussed previously, the wide tuning ranges of QCLs allow for laser PA absorbance spectra of various analytes to be collected. Furthermore, this tuning

ability permits the simultaneous detection of several components in a gas mixture and, if a proper wavelength region is chosen in which the absorption spectral features are clearly identified, increased molecular discrimination. Multivariate analysis permits simultaneous analysis of multiple components and is therefore an attractive tool for distinguishing several analytes based on spectral differences. ARL has used the partial least-squares 2 regression method to develop a model for the simultaneous differentiation of acetic acid, acetone, 1,4-dioxane, and vinyl acetate based on their absorbance features from 1050 to 1240 $cm^{-1}$ (9.52 to 8.06 µm) acquired experimentally using a pulsed Daylight Solutions QCL and a MEMS-scale differential PA cell.[15] The absorption features for these molecules in this wavelength region are assigned to carbon–carbon and carbon–oxygen stretching vibrations. The pulsed source operated at room temperature with passive air cooling. A 21.6-kHz pulse rate provided an average optical power of 1.32 mW. Figure 7 presents the laser PA spectra collected for these species in this wavelength region. For all species, there was excellent agreement between the PA and FTIR spectra (data not shown).

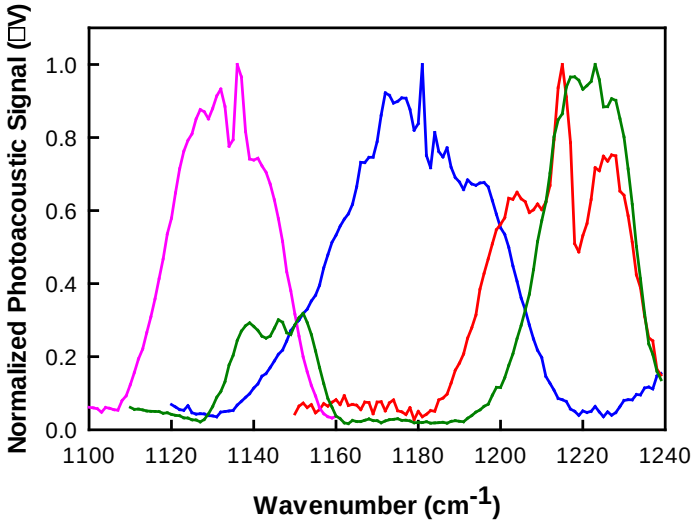


**Fig. 7 Laser PA spectral absorption features of acetic acid (blue), acetone (red), 1,4-dioxane (pink), and vinyl acetate (green)**

We used training samples (PA spectra) having a wide range of analyte concentrations as the basis to develop this model. The model simultaneously uses 4 algorithms, each devoted to the identification of a particular species. It is the concurrent application of the algorithms that facilitates the classification (i.e., identification) of unknown spectra. A model using 1–10 factors or principal components was constructed for the prediction of the analytes of interest. Scores for the first 3 principal components are plotted in Fig. 8. This plot illustrates 4

distinct groups, defined for acetic acid, acetone, 1,4-dioxane, and vinyl acetate. These results confirm that the spectral features of the 4 analytes, and therefore their molecular compositions, are different. Furthermore, segregation of the training spectra into 4 lobes suggests that this model can be used to distinguish these particular species from one another; however, the overlapping lobes suggest the potential for an increased false alarm rate at low concentrations. We evaluated the performance of the model and ability of our QCL-based miniaturized PA sensing platform for the simultaneous detection and discrimination of multiple species. We introduced mixtures composed of known concentrations of the 4 analytes of interest, which were used to challenge the model. The model accurately discriminated between species having similar molecular components and identified specific analytes in mixtures and their concentrations.

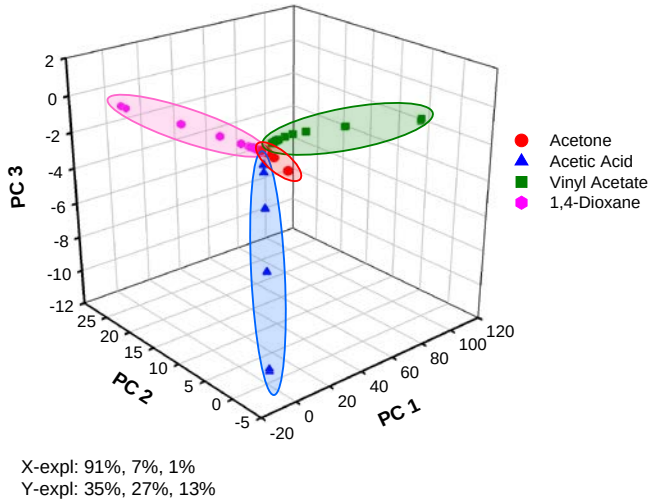


**Fig. 8 Scores plot for the partial least-squares 2 model, using the first 3 calculated principal components. Data points for each analyte are encircled in lobes as a guide to the eye and convey no direct information.**

Most recently, we employed a Pranalytica Q-CW QCL in our MEMS-scale PA gas sensing platform to study acetone. This source allowed us to compare the figures of merit achieved for both pulsed and modulated CW operation. In pulsed mode, the laser was driven externally with an external drive signal source. A 5.0-V, 21.6-kHz transistor-transistor logic (TTL) signal provided an average optical power of 2.70 mW. To achieve modulated CW operation, the Q-CW laser output was modulated by an externally supplied TTL signal. The modulation was imposed on the internal high frequency (1 MHz) drive signal. A function generator was connected to the laser head to allow for external modulation. A 5.0-V, 5.0-kHz TTL signal resulted in 50% modulation and provided an average optical power of

68 mW. In both cases, a compact chiller operating at 17 °C was used for laser cooling. The Pranalytica laser system was equipped with a red guide laser for ease of alignment with the PA cell. Figure 9 shows the PA spectra for acetone, collected using our sensor. The spectrum in Fig. 9a was collected using the QCL in pulsed mode as the laser wavelength was continuously tuned from 7.00 to 8.70 µm (1428 to 1150 $cm^{-1}$), in 0.01-µm (1.5-$cm^{-1}$) increments. The spectrum in Fig. 9b was collected using modulated Q-CW laser operation and continuously tuning over the same wavelength range as before. Acetone has known absorption features in this wavelength range, assigned to carbon–carbon and carbon–oxygen stretching vibrations. The absorbance spectrum for acetone, which was recorded using a FTIR, is also provided in Fig. 9a and b for comparison to the PA data. There is good agreement between the laser PA data and the FTIR spectroscopy absorbance spectrum. The acetone absorbance maximum in the QCL wavelength tuning range is 8.21 µm (1218 $cm^{-1}$). Therefore, this wavelength was used for acetone sensitivity monitoring. Figure 10 illustrates the sensor responses as a function of acetone concentration under (a) pulsed and (b) modulated Q-CW QCL operation. The results exhibit excellent linearity. Minimal detectable acetone concentrations of 172 and 257 ppb were achieved employing pulsed and modulated Q-CW QCL operation, respectively.

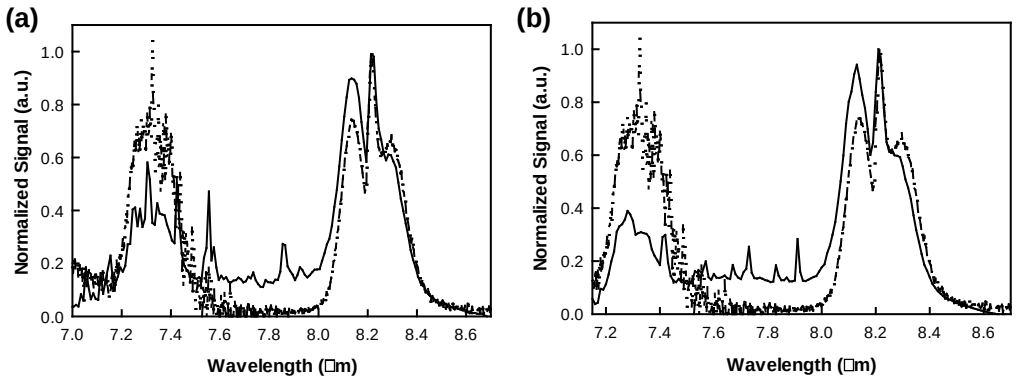


**Fig. 9 Measured a) pulsed and b) modulated Q-CW laser PA spectra (—) of acetone. Data derived from our own PA measurements are compared to FTIR reference spectrum (– –)**

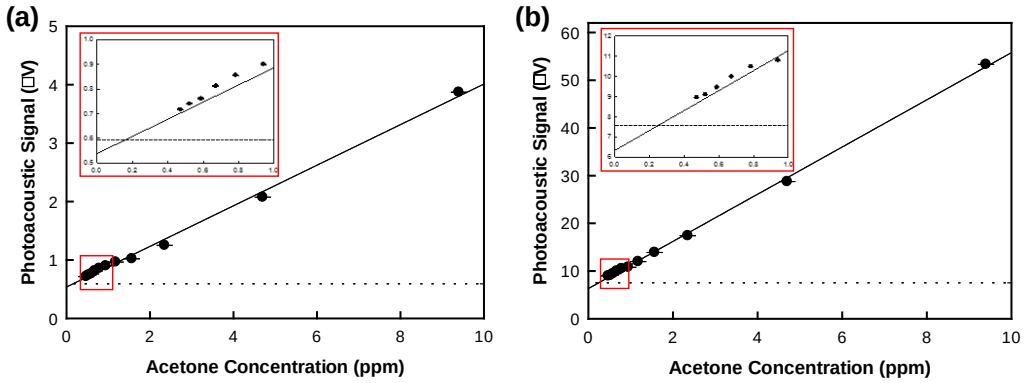


**Fig. 10 PA sensor response as a function of acetone concentration under a) pulsed and b) modulated Q-CW QCL operation. Error bars represent one standard deviation. The dashed line represents 3 standard deviations (3σ) of the background signal. A linear function has been fit to the data. The lower concentration values are inset.**

Our reported LOD for acetone using a similar MEMS-scale PA sensor platform, in which we employed a commercially available pulsed Daylight Solutions EC-QCL, was 555 ppb.[15] In comparison, these most recent results show improved LODs. These improved results were expected, as the average optical power output for the Pranalytica Q-CW QCL, in both modes of operation, was greater than that of the previously employed Daylight Solutions QCL model.

The availability of continuously tunable QCLs having a broad wavelength tuning range makes this an attractive approach for a variety of applications. Employing an array of continuously tunable QCLs in a PA gas sensor would provide a broad wavelength tuning range, allowing for increased molecular discrimination and simultaneous detection of several molecules of interest. As demonstrated by the results summarized earlier and published previously, our PA gas sensing research has benefitted from the broad tuning capabilities of QCLs; however, each laser system we have employed in a PA sensing platform has exhibited limitations. Although the laser element itself is quite small (typically 3–6 mm) in each of the systems discussed here, the packaging, power supply, and controller remain logistical burdens.

As stated earlier and supported in our results, the signal generated from a PA experiment is directly proportional to the absorbed incident power. This power is dependent on the wavelength and output format of the excitation source, which is normally restricted to CW or low-duty cycle pulsed operation. This restriction is directly associated with the inefficiency of the QCL (<10%) and its thermal effect on the feedback mechanisms. The localized heating of the element will change output wavelength and “pull” the laser to mode-hop unless it is pulsed short enough

to avoid large heating or operated in a continuous fashion, which establishes thermal equilibrium. For the pulsed sources evaluated in our laboratory, the duty cycles were as low as 1% and no higher than 5%. These values were dictated by the pulse frequency, which in our PA experiments was slow compared to the manufacturer's optimized specifications. This factor greatly reduced the average power available for our PA sensing experiments. A higher average optical power was achieved using a modulated CW source; however, amplitude modulation of the CW source was not optimal and we were limited to specific current settings due to the mode-hopping nature of the source. These factors reduced our ability to attain a higher average power with this CW QCL model. The highest average optical power was achieved using the externally modulated Q-CW QCL; however, we also observed a higher noise floor when employing this model, resulting in reduced sensitivity.

Comparing the modulated QCLs to the pulsed mode sources under similar experimental conditions (i.e., wavelength, trace gas concentration, frequency), the increased output power of the modulated CW lasers afforded better detection limits compared to the pulsed sources. However, consideration of power consumption and heat management favors the use of a pulsed QCL for future PA gas sensor development. A pulsed QCL with increased optical output power may result in comparable detection limits. In fact, it has been demonstrated and theoretically confirmed that, with respect to modulated operation (optimized for a 50% duty cycle), pulsed laser sources produce $\pi/2$ times higher PA signals under similar experimental conditions and average power.[7]

## 3. Photoacoustic Detection of Condensed-Phase Samples

Investigating solid and liquid materials using the PA technique is attractive as it allows optical absorption measurements to be made for optically opaque samples. This capability of PAS, along with its insensitivity to scattered light, makes this technique a very attractive spectroscopic tool for the investigation of condensed-phase samples.[44–47] PAS in these phases can be accomplished using both a direct or indirect coupling method. The direct coupling method is simple and there have been numerous studies using piezoelectric elements in contact with liquid or solid samples for PA detection.[5,48,49] More recent reports describing PA detection of solid samples use conventional microphones and the indirect coupling method.[47,50] The indirect PA detection of liquids or solids, which has been investigated at ARL,[17] relies on the gas coupling method and is explained by Rosencwaig as the gas-piston model.[51] In this model, the periodic heating of the sample occurs in the absorption length of the sample, but only the heat within a defined diffusion length from the

sample interface can interact with the layer of gas directly above the surface in phase with the excitation light modulation. The periodic expansion in this gas layer produces an acoustic wave that can be detected using standard condenser microphones. The diffusion length is frequency-dependent such that lower modulation or pulse frequencies result in longer diffusion lengths and higher modulation or pulse frequencies result in shorter diffusion lengths.[52] Therefore, PAS of solid samples is often applied to depth profiling of layered samples. Photothermal techniques have proven advantageous for depth profiling as they offer a frequency dependent, and therefore adjustable, probe depth.

Figure 11 depicts a block diagram of the main elements in the ARL platform for PA detection and depth profiling studies of condensed materials. The components and their functionalities are similar to those employed in our gas sensor platform.

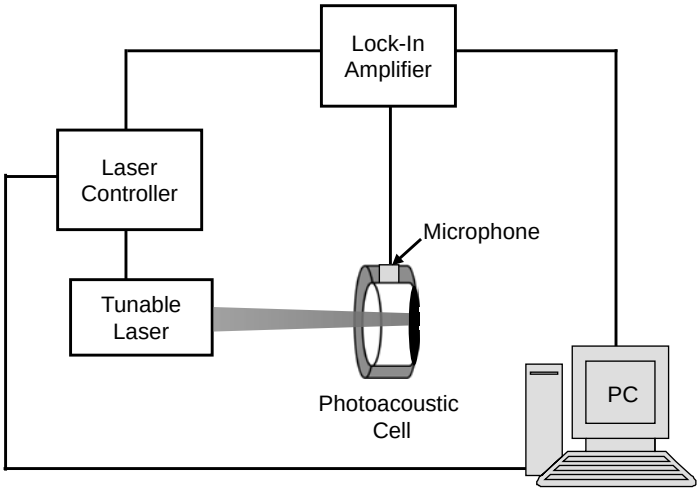


**Fig. 11 Simplified schematic diagram of the ARL PA sensor system for the detection of condensed materials**

## 3.1 Laser Source

Although there have been several reports discussing the use of tunable IR sources, such as QCLs and $CO_2$ lasers, to obtain PA spectra of gases, the application of these sources in PA experiments on condensed-phase samples are minimal. ARL has evaluated pulsed Daylight Solutions QCL technology in the implementation of these sources for PAS for depth profiling investigations of condensed phase materials. Specifically, the ability of the operator to change the pulse frequency (i.e., repetition rate) is an attractive feature for investigating probe depth.

## 3.2 Acoustic Resonator

As discussed previously for acoustic resonators for PA gas sensing, an essential element of a PA sensor for condensed phase sample detection is the cell and optimum design is necessary to facilitate signal generation and detection. ARL designed and fabricated in-house an aluminum cylindrical PA cell to meet our design specifications. The cell consisted of a 4-mm-long resonator with a diameter of 16 mm. The closed cell had a zinc selenide (ZnSe) window on one side of the resonator and the sample substrate material on the other. The cell was equipped with a microphone, which was wired to a power supply (AA battery) and a lock-in amplifier (via a BNC cable). Figure 12a and b provides a simplified illustration and a photograph of the PA cell, respectively.

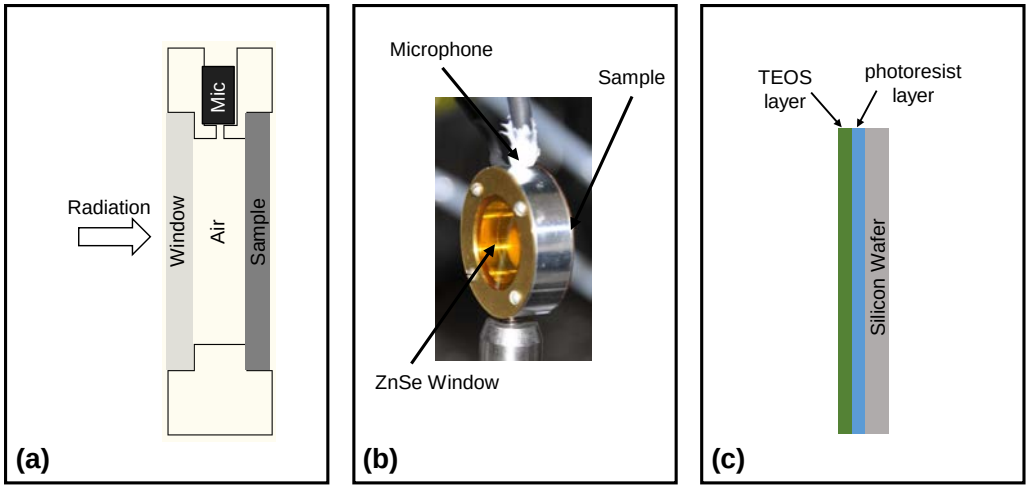


**Fig. 12 a) Basic PA cell components and orientation, b) photograph of the PA cell used when collecting data, and c) sample stack**

The PA cell was designed to have resonance features in the 10- to 40-kHz frequency range, which was limited by the operational range of the microphone. Experimental resonance frequencies of 12.5, 20.9, 26.0, and 36.3 kHz were observed for the cell. These results were in agreement with the predicted theoretical radial resonance frequencies for a cylindrical cavity resonator as described in the literature.[23,36] Amplification of the acoustic signal resulted when the laser pulse frequency was the same as an acoustic resonance frequency of the PA cell.

## 3.3 Application

ARL collected PA spectra for a layered system, illustrated in Fig. 12c, composed of tetraethoxysilane (TEOS) and a photoresist-coated silicon wafer, and

demonstrated discrimination between these compounds and the substrate itself based on sample depth profiling.[17] These materials were chosen specifically for this proof-of-concept demonstration, because each has known absorbance features in the wavelength tuning range of the QCL and the thermal properties for these materials are known. All spectra were collected as the laser was continuously tuned from 1025 to 1240 $cm^{-1}$ (9.76 to 8.06 μm), in 1-$cm^{-1}$ increments. This spectral region is appealing as it contains absorption features representative of vibrational modes present in the selected molecules, specifically, carbon–oxygen, silicon–oxygen, silicon–oxygen–carbon, and silicon–oxygen–silicon stretching vibrations. The source operated at room temperature with passive air cooling. Depending on the pulse repetition rate (ranging from 10.0 to 40.0 kHz), the provided average optical powers ranged from 1.60 to 6.50 mW. In this study, it was useful to compare the position of these features in this wavelength range. Spectral differences among TEOS and photoresist made it possible to distinguish these compounds.

PA spectra were collected for varying thicknesses of TEOS films on a photoresist-coated silicon substrate. Selected spectra are provided in Fig. 13. For each film thickness, spectra were collected at the experimentally determined resonance frequencies (i.e., 12.5, 26.0, and 36.3 kHz). These frequencies resulted in strong PA signals. Depending on the TEOS film thickness, the spectra in Fig. 13 show absorption features characteristic of photoresist and/or TEOS. In general, at the 3 frequencies investigated for the TEOS samples, as the TEOS film thickness was increased, the magnitude of the absorption feature at approximately 1100 $cm^{-1}$ (associated with the silicon–oxygen–silicon stretching vibrations of the TEOS molecules) also increased. The opposite observation can be made for the broad absorption feature centered at approximately 1175 $cm^{-1}$ (associated with the carbon–oxygen stretching vibrations of the photoresist molecules). For thinner TEOS films, the magnitude and appearance of this broad feature were significant; however, as the TEOS film thickness increased, the magnitude of this absorption feature decreased. These results were due to the film thickness approaching the maximum diffusion length (at a given frequency).

To our knowledge, this was the first reported study detailing the development of a PA device employing a single, continuously tunable QCL for depth profiling studies, including discrimination between a material and the substrate on which it is deposited. The availability of continuously tunable QCLs having a broad wavelength and pulse or modulation frequency tuning range makes this an attractive approach for a variety of applications.

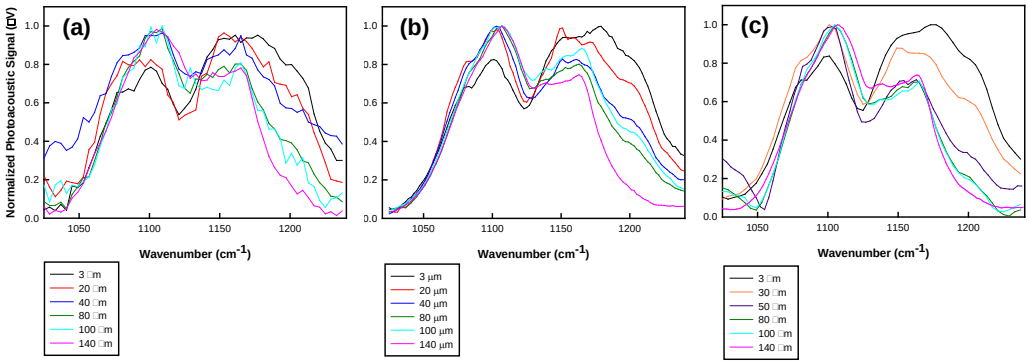


**Fig. 13 Laser PA spectral absorption features for varying thicknesses of TEOS films on a photoresist-coated silicon substrate collected at a) 12.5 kHz, b) 26.0 kHz, and c) 36.3 kHz**

## 4. Standoff Photoacoustic Detection

Standoff detection is desired over contact and proximal methods, because it allows for increased operator safety during the investigation of these hazardous materials. Standoff refers to instances in which the excitation source, detector, and system operator are located at a safe distance from the target samples. The PA effect has not been investigated extensively for standoff explosives detection platforms; most are purely optical (i.e., optical interrogation and optical detection). This is mainly due to the higher sensitivities achieved with in situ PA methods as well as the numerous challenges associated with PAS of samples in open air. In the absence of a sealed PA cell, acoustic waves spread, broadening their already minimal energy below the detection limits of acoustic detectors. Additionally, direct microphone detection is met with difficulty due to the influence of wind effects, such as air turbulence or constant winds.[53] Interferometric sensors are an attractive alternative as they provide high sensitivity over long distances (>300 m) and maintain eye safety.[54] Instead of detecting the acoustic wave directly, these sensors respond to the PA excitation by measuring the total change in optical path length of a coherent light source reflected from the surface of the sample. ARL has investigated an interferometric PA sensor in a standoff spectroscopy experiment using a QCL as the excitation source.[18] Figure 14 depicts a block diagram of the basic elements used in the standoff PA measurements. Shifting from traditional PA cell-based PAS to a standoff method requires modification to the experimental design. The components remain largely the same, with the exception of the amplifying PA cell and the microphone used to measure the pressure fluctuations. Instead, an interferometer (i.e., laser Doppler vibrometer [LDV]) is employed to measure the physical response of the excited system at a standoff distance.

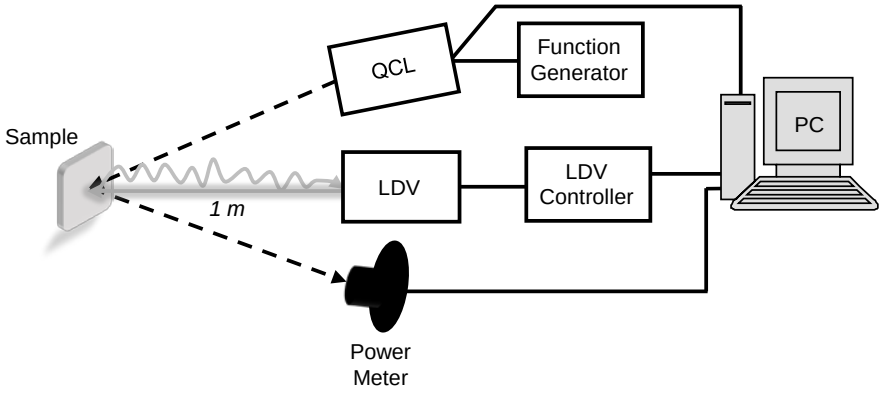


**Fig. 14 Simplified schematic diagram of the ARL PA sensor setup used for the standoff detection of explosives at 1 m**

## 4.1 Laser Source

ARL evaluated a broadly tunable, Pranalytica Q-CW QCL as the excitation source for the standoff PA sensing system. The Q-CW laser produced a train of pulses at a high repetition rate (1 MHz). An external modulation envelope was applied to the train of pulses producing modulated packets of pulses. The laser output was modulated by an externally supplied TTL level (0–5 V, high Z, rising edge synchronization) signal source. The modulation was imposed on the internal high frequency (1 MHz) drive signal. A function generator was connected to the laser head via a BNC connector to allow for external modulation.

## 4.2 Laser Doppler Vibrometer

In place of a traditional microphone detector, a commercial off-the-shelf LDV was employed for standoff PA detection. The LDV can be considered a variant of a Michelson interferometer that records system response to PA excitation by measuring the total change in optical path length of a helium neon (HeNe) laser beam reflected from the surface of the interrogated sample. The HeNe interrogation beam of the LDV must be carefully aligned to reflect from the intersection point of the sample and the excitation source. This alignment is necessary because the LDV measures not just the acoustic disturbance in the gas adjacent to the sample but also the surface motion induced in the sample and substrate system and the changes in index of refraction of the gas boundary as it heats and cools from the excitation. These physical responses in the sample are largest at the intersection point of the excitation source and sample. Measurements are made in the LDV by comparing the time rate of change of the interference of the probe beam that is recombined with and internal reference beam at a photodiode.

## 4.3 Application

ARL collected PA spectra at a standoff distance of 1 m for 3 common military grade explosive hazards; 1,3,5-trinitroperhydro-1,3,5-triazine (RDX), pentaerythritol tetranitrate (PETN), and 2,4,6-trinitrotoluene (TNT).[18] These spectra are shown in Fig. 15. RDX and PETN spectra were collected as the laser was continuously tuned from 7.0 to 8.50 µm (1428 to 1176 $cm^{-1}$), in 0.01-µm (1.5-$cm^{-1}$) increments. TNT spectra were collected as the laser was continuously tuned from 7.20 to 7.70 µm (1389 to 1299 $cm^{-1}$), in 0.01-µm (1.5-$cm^{-1}$) increments. These wavelength tuning ranges were based on known absorption features for these molecules. Specifically, RDX has known absorption features attributed to nitrogen–nitro stretching vibrations, carbon–hydrogen out of plane bending vibrations, and nitrogen–carbon–nitrogen stretching vibrations; PETN has known absorption features assigned to carbon skeletal vibrations, carbon–hydrogen wagging and bending vibrations, and oxygen–nitrogen–oxygen symmetric stretching vibrations; and TNT has known absorption features attributed to carbon–carbon stretching vibrations within the ring structure of the molecule. The source operated at room temperature with passive air cooling. A 5.0-V, 5.0-kHz TTL signal resulted in 50% modulation and provided an average optical power of 68 mW. The laser system was equipped with a red guide laser for ease of alignment, which is invaluable for aligning the HeNe interrogation beam of the LDV with the intersection point of the sample and the excitation source. The absorbance spectra for these explosives, recorded using an FTIR spectrometer equipped with an ATR accessory, are also provided in Fig. 15 for comparison to the PA data. There is very good agreement between the PA and FTIR spectroscopy data. Minor differences were a result of background sources not eliminated during the background collection. The peaks required for substance identification are clearly reproduced in the PA measurements.

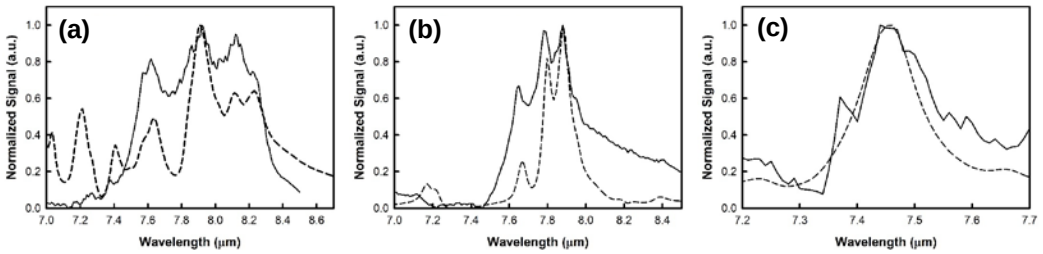


**Fig. 15 Measured Q-CW laser PA spectra of () RDX (—), b) PETN (—), and c) TNT (—). Data derived from our own standoff PA measurements are compared to FTIR reference spectra (– –).**

The concentration of the RDX and TNT samples was 500 µg/$cm^2$ over a 1-$cm^2$ target area. The concentration of the PETN sample was 150 µg/$cm^2$ over a 1-$cm^2$

target area. The explosive samples were prepared using a drop-on-demand inkjet printer. Drop-on-demand inkjet printing was selected over other methods, such as spray deposition or dropcasting, because of the desire to maximize uniformity of the analyte.[55–57] Drop-on-demand sample preparation has been shown to be an effective way to produce uniform samples of controlled quantities for investigation as this sample preparation method allows for the minimization of sample variance as a contributing factor to experimental uncertainty.[58–62]

Substrate interaction is a nontrivial source of signal generated in the interferometric PA detection technique and must be understood in order to reduce the substrate background from the PA signal generated by the analyte of interest. Investigation into substrate response in standoff PAS experiments in our laboratory has shown that there is a major contribution to the signal.[63] We have investigated 2 pathways for substrate interaction and found them both to be significant. Absorption of the excitation source occurs in both the analyte and the substrate, generating PA signal when there is no analyte and amplifying the signal from the system when the analyte is present. Substrate absorption can increase the likelihood of false positive detections when strong substrate response overwhelms analyte signal or obscures the subtle differences between blank and sample. As demonstrated with our proximal PA detection of condensed phase samples, there are beneficial experimental contributions from substrate absorption when performing PA depth profiling experiments. Substrate absorption spectra will differ from that of the analyte, and control of the modulation frequency of the excitation source controls penetration depths within the analyte-substrate system. Confirmation of the substrate response was accomplished via modeling. Assumptions made for model simplification for substrate absorption ignored the second substrate interaction path; the vibrational modes excited in small substrates. Small plate theory was used successfully to confirm experimental results detailing the relationship between substrate dimensions and modal frequencies excited in a PA experiment. Substrate composition also plays a significant role. Using vibrational modes, it is possible that standoff PAS systems can recreate the amplification used in microphone and cell-based PA experiments.

Our results illustrated the capability of this method for detection of explosives at a distance and without the need for a PA cell. The availability of continuously tunable QCLs having a broad wavelength tuning range makes this an attractive approach for a variety of applications, as this method is adaptable to new analytes of interest by changing or adding excitation sources.

## 5. Conclusions and Outlook

The versatility of laser-based PAS for sensing applications has been demonstrated by numerous state-of-the-art examples over the past 45 years. Detection limits for gaseous and condensed media are often in the parts-per-billion or sub-parts-per-billion range, with some reports of parts-per-trillion level sensing capabilities. Furthermore, PA detection schemes are not limited to laboratory measurements and can be used at standoff distances.

The development of continuously tunable sources, such as QCLs, allows for PA spectra to be collected. Data collected with a simple hearing aid microphone have been presented for numerous chemical species and are in excellent agreement with absorption spectra collected for the same analytes using a FTIR spectrometer. Additionally, these broadly tunable sources allow for the simultaneous detection of several molecules of interest as well as increased molecular discrimination.

Although numerous reports have verified the sensitivity of PA sensors at trace levels, the total system size represents a large logistics burden in terms of bulk, cost, and power consumption. ARL's research into PA sensing over more than a decade has taken on many of the issues involved with sensor miniaturization. Our successful demonstration of PA sensing platforms using MEMS-scale PA cells and compact QCLs is an important step toward the development of man-portable sensor systems and we expect continued success from PA-based sensing applications for the detection of a diverse range of chemical agents. ARL recommends continued investment in this technology for trace gas detection at proximal distances.

Although ARL and others have demonstrated the effectiveness of traditional PAS as a spectroscopic tool for the proximal detection and identification if chemical hazards, standoff detection is still an emerging field, and numerous complications exist that make this a very challenging area. For example, the effects of wind conditions or air currents on the acoustic detection may pose a significant problem. Researchers at the University of Maryland Baltimore County have demonstrated direct measurements using a microphone as a detector and the resulting decay of acoustic waves as detection distance increases.[64] Innovative approaches employing the photoacoustic effect for the standoff detection of hazards are under investigation and show potential for overcoming many of the challenges. Although the acoustic waves generated at standoff distances are affected by atmospheric conditions, the reflected or scattered light is not. Employing a quartz crystal tuning fork (QCTF), researchers at Oak Ridge National Laboratory demonstrated a standoff PAS technique using the laser light reflected or scattered off the target material.[53,65–67] The scattered/reflected light was collected using a spherical mirror and focused

onto a QCTF, producing an acoustic wave and driving the QCTF into resonance. The light stimulating the QCTF is diminished by the amount absorbed by the target, and the contribution of the residue is determined by subtraction of the substrate background. Using this technique, the reported sensitive and selective detection of a variety of surface-adsorbed compounds. Researchers at Laser Science and Technology Center in India have developed a portable explosives detection system based on the QCTF PA technique for field applications.[68] In general, an initial background spectrum must be collected to remove the absorption effects not produced by the target material. Therefore, the properties of background materials might affect the ability QCTF PA signals to discriminate between chemical species and the substrates; thus, various types of substrate material that might be encountered should be thoroughly investigated.

Recently, researchers at the Massachusetts Institute of Technology Lincoln Laboratory developed a modular, standoff, laser-induced acoustics system to detect and discriminate trace amounts of explosive material.[69] Photoacoustic sensing of explosives (PHASE) exploits PA phenomena resulting from UV laser excitation. Exposed explosives are excited using an UV laser. The high peak power of this laser causes explosives to dissociate, vaporize, and release into the near atmosphere, producing intense local pressure variances and resultant acoustic signals. PHASE uses laser vibrometry to remotely measure photoacoustic emissions, enabling long standoff sensing. Photoacoustic signals from explosive hazards differed significantly from background materials (e.g., soil, concrete, metal, clothing/fabric) allowing PHASE to observe explosives versus common background materials with high detection probabilities and low false-alarm rates.

The future of PAS for sensing applications includes the continued development of laser sources with respect to broad tunability and decreased system sizes and power requirements. Daylight Solutions now offers a compact, rapid-scan CW-pulsed mid-IR QCL with up to 400 $cm^{-1}$ wavelength tunability.[70] Pendar Technologies is developing monolithic QCL arrays to create a high-power, mid-IR laser in a small package.[71] Pendar's QCL arrays have advanced to the point of realizable inclusion in a miniaturized photoacoustic sensor platform, offering a unique synergetic concept with no moving parts, broad wavelength coverage, and rapid commercial scalability (electronics, III-V lasers, and MEMS-scale PA cell and microphone). We believe that as leading QCL manufacturers continue to push the envelope in laser development for a variety of applications, most, if not all, of the desired operational capabilities will be realized in the near future, allowing for commercialization of PA chemical sensors for deployment as wearables and for use in sensor networks.

## 6. Funding

This work was supported in part by appointments to ARL's Postdoctoral Fellowship Program administered by the Oak Ridge Associated Universities through a contract with ARL.

## 7. References


1. Bijnen FGC, Reuss J, Harren FJM. Geometrical optimization of a longitudinal resonant photoacoustic cell for sensitive and fast trace gas detection. Rev Sci Instrum. 1996;67(8):2914–2923.

2. Nagele M, Sigrist MW. Mobile laser spectrometer with novel resonant multipass photoacoustic cell for trace-gas sensing. Appl Phys B. 2001;70:895–901.

3. Bialkowski SE. Photothermal spectroscopy methods for chemical analysis. New York (NY): John Wiley & Sons; 1996. (Vol. 134).

4. Kinney JB, Staley RH. Applications of photoacoustic spectroscopy. Ann Rev Mater Sci. 1982;12:295–321.

5. Patel CKN, Tam AC. Pulsed optoacoustic spectroscopy of condensed matter. Rev Mod Phys. 1981:53(3):517–550.

6. Tam AC., Applications of photoacoustic sensing techniques. Rev Mod Phys. 1986;58(2):381–431.

7. Bartlome R, Kaucikas M, Sigrist MW. Modulated resonant versus pulsed resonant photoacoustics in trace gas detection. Appl Phys B. 2009;96:561–566.

8. Miklós A, Hess P., Modulated and pulsed photoacoustics in trace gas analysis. Anal Chem. 2000;72:30A–37A.

9. Faist J, Capasso F, Sivco DL, Sirtori C, Hutchinson AL, Cho AY. Quantum cascade laser. Science 1994;264(5158):553–556.

10. Mandelis A, Hess P. Progress in photothermal and photoacoustic science and technology: life and earth sciences. Bellingham (WA): SPIE–The International Society for Optical Engineering; 1997; Vol. 3.

11. Michaelian KH. Photoacoustic infrared spectroscopy. Hoboken (NJ): Wiley-Interscience; 2003.

12. Rosencwaig A. Photoacoustics and photoacoustic spectroscopy. New York (NY): John Wiley & Sons; 1980.

13. Sigrist MW. Air monitoring by laser photoacoustic spectroscopy. In Air monitoring by spectroscopic techniques, Sigrist MW, editor. New York (NY): Wiley Interscience; 1994. (Vol. 127).

14. Tam AC. Photoacoustics: spectroscopy and other applications. In Ultrasensitive laser spectroscopy. Klinger DS, editor. New York (NY): Academic Press; 1983.

15. Holthoff E, Bender J, Pellegrino P, Fisher A. Quantum cascade laser-based photoacoustic spectroscopy for trace vapor detection and molecular discrimination. Sensors. 2010;10:1986–2002.

16. Holthoff EL, Heaps DA, Pellegrino PM. Development of a MEMS-scale photoacoustic chemical sensor using a quantum cascade laser. IEEE Sens J. 2010;10(3):572–577.

17. Holthoff EL, Marcus LS, Pellegrino PM. Quantum cascade laser based photoacoustic spectroscopy for depth profiling investigations of condensed-phase materials. Appl Spectrosc. 2012;66(9):987–992.

18. Marcus LS, Holthoff EL. Pellegrino PM. Standoff photoacoustic spectroscopy of explosives. Appl Spectrosc. 2016 Jun 24.

19. Kauppinen J, Wilcken K, Kauppinen I, Koskinen V. High sensitivity in gas analysis with photoacoustic detection. Microchem J. 2004;76(1–2):151–159.

20. Koskinen V, Fonsen J, Roth K, Kauppinen J. Progress in cantilever enhanced photoacoustic spectroscopy. Vib Spectrosc. 2008;48(1):16–21.

21. Kosterev AA, Tittel FK, Serebryakov DV, Malinovsky AL, Morozov IV. Applications of quartz tuning forks in spectroscopic gas sensing. Rev Sci Instrum. 2005;76(4):043105-1-9.

22. Harren FJM, Bijnen FGC, Reuss J, Voesenek L, Blom C. Sensitive intracavity photoacoustic measurements with a CO2 wave-guide laser. ApplPhyss B-Photophysics and Laser Chem. 1990;50(2):137–144.

23. Miklós A, Hess P, Bozoki Z. Application of acoustic resonators in photoacoustic trace gas analysis and metrology. Rev Sci Instrum. 2001;72(4),:1937–1955.

24. Rosengren LG. Optimal optoacoustic detector design. Appl Optics. 1975;14(8):1960–1976.

25. Pellegrino PM, Polcawich RG. Advancement of a MEMS photoacoustic chemical sensor. Proc SPIE. 2003;5085:52–63.

26. Firebaugh SL, Jensen KF, Schmidt MA. Miniaturization and integration of photoacoustic detection with a microfabricated chemical reactor system. JMEMS. 2001;10:232–237.

27. Firebaugh SL, Jensen KF, Schmidt MA. Miniaturization and integration of photoacoustic detection. J Appl Phys. 2002;92:1555–1563.

28. Heaps DA, Pellegrino P. Examination of a quantum cascade laser source for a MEMS-scale photoacoustic chemical sensor. Proc SPIE. 2006;6218:621805-1-621805-9.

29. Heaps DA, Pellegrino P. Investigations of intraband quantum cascade laser source for a MEMS-scale photoacoustic sensor. Proc SPIE. 2007;6554:65540F-1-65540F-9.

30. Pellegrino PM, Polcawich RG, Firebaugh SL. Miniature photoacoustic chemical sensor using microelectromechanical structures. Proc SPIE. 2004;5416(1):42–53.

31. Miklós A, Hess P, Mohacsi A, Sneide J, Kamm S, Schafer S. Improved photoacoustic detector for monitoring polar molecules such as ammonia with a 1.53 μm DFB diode laser. AIP Conf Proc. 1999;(463):126–128.

32. Leugers MA, Atkinson GH. Quantitative-determination of acetaldehyde by pulsed laser photoacoustic-spectroscopy. Anal Chem. 1984;56(6):925–929.

33. Miklós A, Brand C, Winkler A, Hess P. Effective noise-reduction on pulsed-laser excitation of modes in a high-Q photoacoustic resonator. J Phys IV 1994;4(C7):781–784.

34. Schafer S, Miklós A, HessP. Quantitative signal analysis in pulsed resonant photoacoustics. Appl Optics. 1997;36(15):3202–3211.

35. Schafer S, Miklós A, Pusel A, Hess P. Absolute measurement of gas concentrations and saturation behavior in pulsed photoacoustics. Chem Phys Lett. 1998;285(3–4):235–239.

36. Dewey CF. Jr., Desing of optoacoustic system. In Optoacoustic spectroscopy and detection. Pao Y-H, editor. New York (NY): Academic Press; 1977.

37. Karbach A, Hess P. High precision acoustic spectroscopy by laser excitation of resonator modes. J Chem Phys. 1985;83:1075–1084.

38. Miklós A, Lorincz A. Windowless resonant acoustic chamber for laser-photoacoustic applications. Appl Phys B-Photophysics and Laser Chem. 1989;48(3):213–218.

39. Bernegger S, Sigrist MW. Longitudinal resonant spectrophone for CO-laser photoacoustic spectroscopy. Appl Phys. B. 1987;44:125–132.

40. Schill JF, Holthoff EL, Pellegrino PM. Predicting the resonant frequency of photoacoustic cells with side branches. IEEE Sens J. 2015;15(3):1336–1337.

41. Heumier TA, Carlsten JL. App note 8: Mode hopping in semiconductor lasers. Bozeman (MT): ILX Lightwave Corporation; 2016.

42. Holthoff EL, Bender JS, Pellegrino PM, Fisher A, Stoffel N. Photoacoustic spectroscopy for trace vapor detection and molecular discrimination. Proc SPIE. 2010;7665:766510-1-7.

43. Holthoff EL, Marcus LS, Pellegrino PM., Towards the realization of a MEMS-based photoacoustic chemical using ultracompact EC-QCL (SpriteIR). Proc IEEE Sensors. 2013:1–4.

44. Chaudhary AK, Bhar GC, Da, S. Low-limit photo-acoustic detection of solid RDX and TNT explosives with carbon dioxide laser. J Appl Spectrosc. 2006;73(1):123–129.

45. Petzold A, Niessner R. Photoacoustic soot sensor for in-situ black carbon monitoring. Appl Phys B-Lasers Opt. 1996;63(2):191–197.

46. Van Neste CW, Morales-Rodriguez ME, Senesac LR, Mahajan SM, Thundat T. Quartz crystal tuning fork photoacoustic point sensing. Sens Actuator B-Chem. 2010;150(1):402–405.

47. Wen Q, Michaelian KH. Mid-infrared photoacoustic spectroscopy of solids using an external-cavity quantum-cascade laser. Opt Lett. 2008;33(16):1875–1877.

48. Farrow MM, Burnham RK, Auzanneau M, Olsen SL, Purdie N, Eyring EM. Piezoelectric detection of photoacoustic signals. Appl Optics. 1978;17(7):1093–1098.

49. Hordvik A, Schlossberg H. Photoacoustic technique for determining optical-absorption coefficients in solids. Appl Optics. 1977;16(1):101–107.

50. Rabasovic MD, Nikolic MG, Dramicanin MD, Franko M, Markushev DD. Low-cost, portable photoacoustic setup for solid samples. Meas Sci Technol. 2009;20(9):095902-1-6.

51. Rosencwaig A, Gersho A. Theory of photoacoustic effect with solids. J Appl Phys. 1976;47(1):64–69.

52. De Albuquerque JE, Balogh DT, Faria RM. Quantitative depth profile study of polyaniline films by photothermal spectroscopies. Appl Phys A-Mater Sci. Process. 2007;86(3):395–401.

53. Van Neste CW, Senesac LR, Thundat T. Standoff photoacoustic spectroscopy. Appl Phys Lett. 2008;92:234102-1-234102-3.

54. Calasso IG, Sigrist MW. Selection criteria for microphones used in pulsed nonresonant gas-phase photoacoustics. Rev Sci Instrum. 1999;70(12):4569–4578.

55. Holthoff EL, Farrell ME, Pellegrino PM. Investigating a drop-on-demand microdispenser for standardized sample preparation. Proc SPIE. 2012;8358:83580V-1-83580V-8.

56. Holthoff EL, Farrell ME, Pellegrino PM. Standardized sample preparation using a drop-on-demand printing platform. Sensors. 2013;13:5814–5825.

57. Yasuda K, Woodka M, Polcha M, Pinkham D. Reproducible deposition of trace explosives onto surfaces for test standards generation. Fort Belvoir (VA): Night Vision and. Electronic Sensors Directorate; 2010. Report No.: RDER-NV-TR-265.

58. Baeg KJ, Khim D, Kim JH, Kang M, You IK, Kim DY, Noh YY. Improved performance uniformity of inkjet printed n-channel organic field-effect transistors and complementary inverters. Org Electron. 2011;12(4):634–640.

59. Bloom, A. N.; Gillen, G.; Najarro, M.; Windsor, E., Inkjet printed explosive standards. Abstr Pap Am Chem Soc. 2009;237:204–204.

60. Farrell ME, Holthoff EL, Pellegrino PM. Surface enhanced Raman scattering (SERS) detection of ammonium nitrate (AN) samples fabricated using drop-on-demand inkjet technology. Appl Spectrosc. 2014;68(3):287–296.

61. Windsor E, Najarro M, Bloom A, Benner B, Fletcher R, Lareau R, Gillen G. Application of inkjet printing technology to produce test materials of 1,3,5-trinitro-1,3,5-triazcyclohexane for trace explosive analysis. Anal Chem. 2010;82:8519–8524.

62. Yeonjun O, Jihoon K, Young Joon Y, Hyotae K, Ho Gyu Y, Sung-Nam L, Jonghee K. Inkjet printing of $Al_2O_3$ dots, lines, and films: From uniform dots to uniform films. Curr Appl Phys. 2011;11(3):S359–S363.

63. Marcus LS, Holthoff L, Pellegrino PM. Photoacoustic chemical sensing: layered systems and exciation source analysis. Proc SPIE. 2015;9455:94550T-1-T-9.

64. Chen X, Guo D, Choa F-S, Wang C-C, Trivedi S,Fan J. Quantum cascade laser based standoff photoacoustic detection of explosives using ultra-sensitive microphone and sound reflector. Proc SPIE. 2013;8631:86312H-1-86312H-6.

65. Van Neste CW, Senesac LR. Thundat T. Standoff spectroscopy of surface adsorbed chemicals. Anal Chem. 2009;81:1952–1956.

66. Liu X, Van Neste CW, Gupta M, Tsui YY, Kim S, Thundat T. Standoff reflection-absorption spectra of surface adsorbed explosives measured with pulsed quantum cascade lasers. Sens Actuators B. 2014;191:450–456.

67. Morales-Rodriguez ME, Van Neste CW, Senesac LR, Mahajan SM, Thundat T. Ultraviolet decomposition of surface adsorbed explosives investigated with infrared standoff spectroscopy. Sens Actuators B. 2012;161:961–966.

68. Sharma RC, Kumar D, Bhardwaj N, Gupta S, Chandra H, Maini AK. Portable detection system for standoff sensing of explosives and hazardous materials. Opt Commun. 2013;309:44–49.

69. Photoacoustic Sensing of Explosives Tech Notes. Lexington (MA): Communications and Community Outreach Office, MIT Lincoln Laboratory; 2013 Nov [accessed 2016 Aug 29]. https://www.ll.mit.edu/publications/technotes/TechNote_PHASE.pdf.

70. Hedgehog. San Diego (CA): Daylight Solutions; n.d. [accessed 2016 Aug 25]. http://www.daylightsolutions.com/assets/006/5608.pdf.

71. High power MWIR and LWIR QCLs. Cambridge (MA): Pendar Technologies; 2016 [accessed 2016 Aug 25]. http://www.pendartechnologies.com/energy.html.

## List of Symbols, Abbreviations, and Acronyms

| | |
|---|---|
| ARL | US Army Research Laboratory |
| $CO_2$ | carbon dioxide |
| CW | continuous wave |
| DMMP | dimethyl methyl phosphonate |
| EC | external cavity |
| FTIR | Fourier transform IR |
| Ge | germanium |
| HeNe | helium neon |
| IR | infrared |
| LDV | laser Doppler vibrometer |
| LOD | limit of detection |
| MEMS | microelectromechanical systems |
| PA | photoacoustic |
| PAS | photoacoustic spectroscopy |
| PETN | pentaerythritol tetranitrate |
| PHASE | photoacoustic sensing of explosives |
| PTD | photothermal deflection |
| PTI | photothermal interferometry |
| PTL | photothermal lensing |
| QCL | quantum cascade laser |
| Q-CW | quasi-continuous wave |
| QCTF | quartz crystal tuning fork |
| RDX | 1,3,5-trinitroperhydro-1,3,5-triazine |
| SNR | signal-to-noise ratio |
| TEOS | tetraethoxysilane |

| | |
|---|---|
| TNT | 2,4,6-trinitrotoluene |
| TTL | transistor-transistor logic |
| ZnSe | zinc selenide |
| UV | ultraviolet |

1 (PDF) DEFENSE TECHNICAL INFORMATION CTR DTIC OCA

2 (PDF) DIRECTOR US ARMY RESEARCH LAB RDRL CIO L IMAL HRA MAIL & RECORDS MGMT

1 (PDF) GOVT PRINTG OFC A MALHOTRA

1 (PDF) US ARMY EDGEWOOD CHEMICAL BIOLOGICAL CTR RDCB DR A FOUNTAIN

2 (PDF) DIRECTOR US ARMY RESEARCH LAB RDRL SEE VERONICA ATKINSON RDRL SEE E ELLEN L HOLTHOFF PAUL M PELLEGRINO